



# Mathematical problems and methods in resistivity well-loggings

T.T. Li, Y. Tan

## ► To cite this version:

T.T. Li, Y. Tan. Mathematical problems and methods in resistivity well-loggings. RR-2195, INRIA. 1994. inria-00074476

**HAL Id: inria-00074476**

**<https://inria.hal.science/inria-00074476>**

Submitted on 24 May 2006

**HAL** is a multi-disciplinary open access archive for the deposit and dissemination of scientific research documents, whether they are published or not. The documents may come from teaching and research institutions in France or abroad, or from public or private research centers.

L'archive ouverte pluridisciplinaire **HAL**, est destinée au dépôt et à la diffusion de documents scientifiques de niveau recherche, publiés ou non, émanant des établissements d'enseignement et de recherche français ou étrangers, des laboratoires publics ou privés.



INSTITUT NATIONAL DE RECHERCHE EN INFORMATIQUE ET EN AUTOMATIQUE

***Mathematical Problems  
and Methods in Resistivity  
Well-Loggings***

Ta-Tsien LI  
Yongji TAN

N° 2195  
Février 1994

PROGRAMME 6

Calcul scientifique,  
modélisation et  
logiciels numériques

**R***apport  
de recherche*

1994

# Mathematical Problems and Methods in Resistivity Well-loggings

Li Ta-Tsien    Tan Yongji

Dept. of Mathematics, Fudan University, Shanghai 200433, China

**Summary** – The resistivity well-logging is one of the most important and common techniques in petroleum exploitation. In this paper the authors introduce a new kind of boundary value problem, the total flux boundary value problem, to model various resistivity well-logging problems, and review some effective theoretical and numerical techniques to handle this kind of problem.

**AMS Subject Classifications** : 86A20, 35J20, 34B40, 35B27, 35R30.

**Keywords** : Resistivity well-logging ; Total flux boundary problem ; Boundary homogenization.

## Problèmes et Méthodes Mathématiques pour la Diagraphie de Puits par Résistivité

**Résumé** – La diagraphie de puits par résistivité est une des techniques les plus importantes et les plus utilisées en exploitation pétrolière. Dans cet article, les auteurs introduisent une nouvelle sorte de problèmes aux limites, le problème aux limites avec condition de flux total, pour modéliser divers problèmes de diagraphie de puits par résistivité, et ils présentent certaines techniques théoriques et numériques efficaces permettant de traiter ce genre de problème.

**Mots-clés** : Diagraphie de puits par résistivité ; Problème aux limites avec condition de flux total ; Homogénéisation frontière.

# 1 Introduction

In petroleum exploitation one often uses various methods of well-loggings, among which the resistivity well-logging is one of the most important and common techniques. After a well has been drilled, one puts a log tool into the well. The tool discharges a steady current to the underground and forms a static electric field. By measuring the electric potential somewhere, one infers the resistivity of the geological stratum. Combining this information with the porosity of the stratum obtained by some other well-logging techniques, one can calculate the oil storage.

In order to infer the resistivity of the stratum from the well-logging information, we have to determine the corresponding electric field and then to interpret the well-logging information. This asks us to study some interesting mathematical problems. In this paper we shall review the mathematical problems related to the resistivity well-logging, some techniques to solve these problems and certain theoretical aspects.

In section 2, we shall model the resistivity well-logging problem by means of a new kind of boundary value problem, the total flux boundary value problem. In section 3 we set up the variational principle for such boundary value problems and discuss the existence and uniqueness of the solution. In section 4, the procedure for solving this kind of boundary value problem by finite element method will be given. In section 5 we give some numerical results. In section 6 we show the advantages of this mathematical model and describe the limiting behavior of the solution. In section 7 we discuss the boundary homogenization for the boundary value problem. In section 8 and section 9 the inverse problems of resistivity identification and the boundary homogenization for them have been described. In section 10 we present the generalization and applications to some other fields.

## 2 Mathematical modelling for resistivity well-loggings

There are many different kinds of resistivity well-loggings. Without loss of generality, we shall only give the models for the dual-lateral well-logging and the micro-spheric focusing well-logging.

### 2.1 Formation Model

In oil-geophysics [1-2], the underground formation is usually supposed to be regularly stratified. In figure 2.1 a cross section through the well-axis is shown, where  $\Omega_m$  is the well-bore filled with mud;  $\Omega_s$  is the enclosing rock;  $\Omega_{xo}$  and  $\Omega_t$  are two parts of the objective formation, which is the main measuring object. Since the objective formation is usually composed of porous sand-stone, the mud-filtrate penetrates into the porous region and changes the resistivity in the subdomain  $\Omega_{xo}$  which is then called the invaded zone. The part of objective formation which is not invaded by the mud-filtrate is denoted by  $\Omega_t$ .

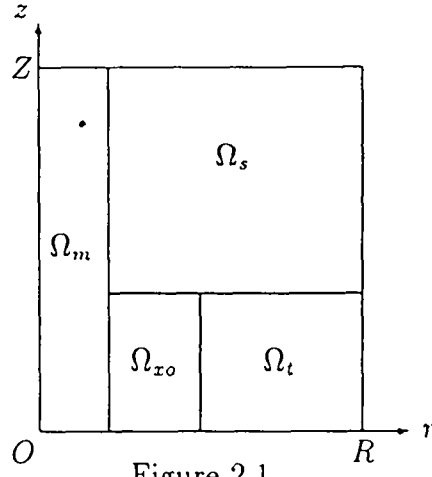


Figure 2.1

The formation is often supposed to be symmetric to the middle plane of the objective formation and to the well-axis.

Since the current discharged from the electrode essentially covers a limited region, usually we limit ourselves to investigate the electric field in the following cylinder

$$\begin{cases} 0 \leq r \leq R, \\ 0 \leq z \leq Z, \end{cases} \quad (2.1)$$

where

$$r = (x^2 + y^2)^{1/2} \quad (2.2)$$

and  $R, Z$  are sufficiently large.

The resistivity function is usually supposed to be piecewise constant:

$$\rho = \begin{cases} R_m & \text{in } \Omega_m, \\ R_{xo} & \text{in } \Omega_{xo}, \\ R_s & \text{in } \Omega_s, \\ R_t & \text{in } \Omega_t. \end{cases} \quad (2.3)$$

For some kinds of resistivity well-loggings, e.g., for the micro-spheric focusing well-logging, the current actually covers a very small domain, then we can neglect the enclosing rock and the objective formation without being invaded by the mud-filtrate and then only investigate the domain composed of the well-bore and the invaded zone. In this case, to detect the resistivity of the invaded zone more accurately we have to consider the mud-cake (with resistivity  $R_{mc}$ ) attached to the well-wall, the generation of which is due to the deposition of the mud. A cross section of the domain through the well-axis is shown in Fig.2.2 and the resistivity function can be written as

$$\rho = \begin{cases} R_m & \text{in } \Omega_m, \\ R_{mc} & \text{in } \Omega_{mc}, \\ R_{xo} & \text{in } \Omega_{xo}. \end{cases} \quad (2.4)$$

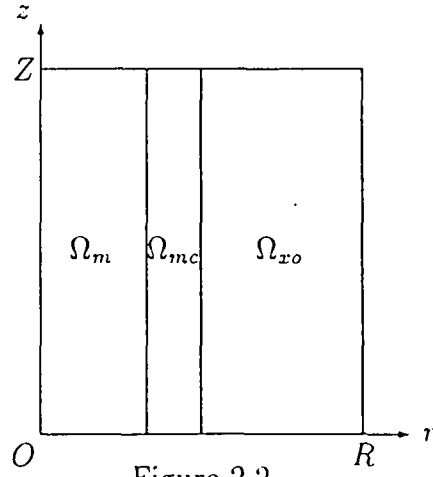


Figure 2.2

## 2.2 Differential equation and boundary conditions

The electric field produced by the resistivity well-logging is approximately a steady one. Let  $u = u(x, y, z)$  be the potential of the electric field. We shall introduce the differential equation and the boundary conditions for it.

In a static electric field without source, the current density function  $\vec{j}$  satisfies the continuity equation

$$\operatorname{div} \vec{j} = 0. \quad (2.5)$$

By Ohm's law in differential form

$$\vec{j} = \frac{\vec{E}}{\rho}, \quad (2.6)$$

where  $\rho$  is the resistivity and  $\vec{E}$  is the intensity of electric field with

$$\vec{E} = -\operatorname{grad} u. \quad (2.7)$$

Therefore we have

$$-\operatorname{div}\left(\frac{1}{\rho} \operatorname{grad} u\right) = 0, \quad (2.8)$$

i.e.

$$-\frac{\partial}{\partial x}\left(\frac{1}{\rho} \frac{\partial u}{\partial x}\right) - \frac{\partial}{\partial y}\left(\frac{1}{\rho} \frac{\partial u}{\partial y}\right) - \frac{\partial}{\partial z}\left(\frac{1}{\rho} \frac{\partial u}{\partial z}\right) = 0. \quad (2.9)$$

It means that the potential function  $u$  satisfies a quasi-harmonic equation. Since  $\rho$  is piecewise constant, the preceding equation must be satisfied in each subdomain where  $\rho$  is a constant.

On each interface of the subdomains with different resistivity, we have to prescribe the corresponding interface conditions. Let  $\Gamma_c$  be one interface,  $\rho_-$ ,  $u_-$

and  $\rho_+$ ,  $u_+$  be the resistivity and the potential on both sides of the interface respectively. By the continuity of potential, at each point of the interface  $\Gamma_c$ , we have

$$u_-|_{\Gamma_c} = u_+|_{\Gamma_c}. \quad (2.10)$$

The current through a surface element  $dS$  on  $\Gamma_c$  is

$$dI = \vec{j} \cdot \vec{n} dS = \frac{1}{\rho} \vec{E} \cdot \vec{n} dS = -\frac{1}{\rho} \frac{\partial u}{\partial n} dS, \quad (2.11)$$

where  $\vec{n}$  is the unit normal vector on  $\Gamma_c$ . By the continuity of current, at each point of the interface  $\Gamma_c$  we have

$$\frac{1}{\rho_-} \left( \frac{\partial u}{\partial n} \right)_- \Big|_{\Gamma_c} = \frac{1}{\rho_+} \left( \frac{\partial u}{\partial n} \right)_+ \Big|_{\Gamma_c}, \quad (2.12)$$

where the normal vector  $\vec{n}$  takes the same direction on both sides of  $\Gamma_c$ , and  $(\frac{\partial u}{\partial n})_+|_{\Gamma_c}$  and  $(\frac{\partial u}{\partial n})_-|_{\Gamma_c}$  stand for the normal derivatives on both sides of  $\Gamma_c$  respectively.

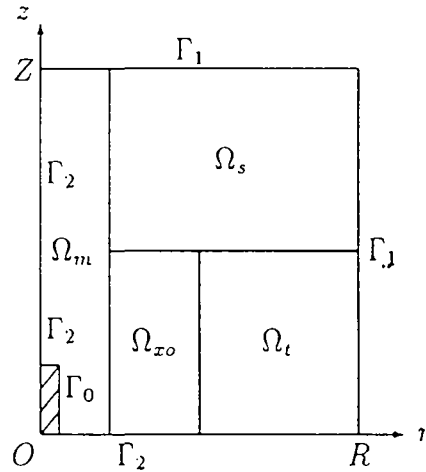


Figure 2.3

On the boundary of the domain (see Figure 2.3), the potential function satisfies several different kinds of boundary conditions. In the case that the potential on  $\Gamma_1$ , a part of the boundary, is known, we have the usual boundary condition of Dirichlet type

$$u|_{\Gamma_1} = f \text{ (given function)}. \quad (2.13)$$

In particular, on the surface of the earth the potential can be assumed to be zero:

$$u = 0; \quad (2.14)$$

moreover, on the boundary far from the electrode, since the electric potential is very weak there, we may also suppose that condition (2.14) is satisfied on it.

On the insulation boundary and the symmetric surface, denoted by  $\Gamma_2$ , we have

$$\vec{j} \cdot \vec{n} |_{\Gamma_2} = -\frac{1}{\rho} \frac{\partial u}{\partial n} \Big|_{\Gamma_2} = 0, \quad (2.15)$$

i.e., the boundary condition of Neumann type

$$\frac{1}{\rho} \frac{\partial u}{\partial n} \Big|_{\Gamma_2} = 0. \quad (2.16)$$

In the resistivity well-logging, some part of the boundary is composed of the metal surfaces of the electrodes. On the metal surface of each electrode, denoted by  $\Gamma_0$ , the potential is unknown but should be constant, i.e.,

$$u |_{\Gamma_0} = \text{const}(\text{to be determined}), \quad (2.17)$$

while the current  $I$  discharged from the electrode is known:

$$\int \int_{\Gamma_0} \vec{j} \cdot \vec{n} dS = \int \int_{\Gamma_0} \frac{1}{\rho} \vec{E} \cdot \vec{n} dS = I \text{ (given constant)}, \quad (2.18)$$

then we have

$$-\int \int_{\Gamma_0} \frac{1}{\rho} \frac{\partial u}{\partial n} dS = I, \quad (2.19)$$

where  $\vec{n}$  is the unit outward normal vector.

By combining (2.17) and (2.19), we get the following boundary condition of new type [3-4]

$$\begin{cases} u |_{\Gamma_0} = c \text{ (unknown constant)}, \\ -\int \int_{\Gamma_0} \frac{1}{\rho} \frac{\partial u}{\partial n} dS = I \text{ (given constant)}, \end{cases} \quad (2.20)$$

called *the boundary condition with equivalued surface* or *the total flux boundary condition*, which is of essential importance in the resistivity well-logging.

### 2.3 Mathematical modelling

To detect the resistivity of the formation by the well-logging measuring information is an inverse problem. Nevertheless, since the corresponding direct problem is the basis for solving the inverse problem, we shall first establish the mathematical model for the direct problem under the assumption that the geometric structure of the formation and the resistivity  $\rho$  are all known, then we discuss the inverse problem.



### 2.3.1 Dual-lateral well-logging

The dual-lateral well-logging [5] is an important technique and has been widely used. The tool of the well-logging is mainly made of an electrode system with nine metal electrode rings embedded into a cylindrical insulator, among which the electrode  $A_0$  is called the *main electrode*; two pairs of electrodes ( $M_1, M_2$ ) and ( $N_1, N_2$ ) are called the *supervision electrodes*; two pairs of electrodes ( $A_1, A_2$ ) and ( $A'_1, A'_2$ ) are called the *screen electrodes* (see Figure 2.4). Two electrodes in each pair are located symmetrically with respect to the main electrode  $A_0$  and are linked each other by wire. There are two kinds of dual-lateral well-loggings: the *deep detection* and the *shallow detection*. Without loss of generality, we only formulate the mathematical model for the deep detection (see the left part of Figure 2.4).

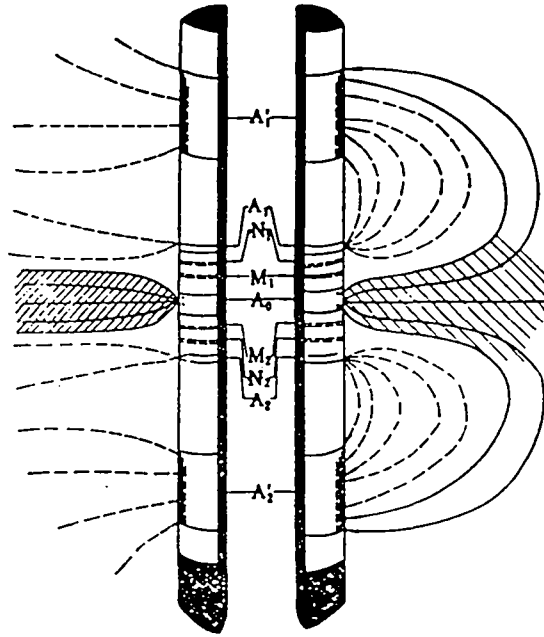


Figure 2.4

In the case of deep detection, the log tool is put in the center of the well and a current  $I_0$ , called the *main current*, is discharged from the main electrode  $A_0$ ; in the meantime, currents  $I_1$  and  $I'_1$  with the same sign as  $I_0$ , called the *screen currents*, are discharged from the pairs of screen electrodes ( $A_1, A_2$ ) and ( $A'_1, A'_2$ ) respectively. Certain circuits can be used to automatically adjust  $I_1$  and  $I'_1$  such that

$$u|_{A'_i} = \gamma u|_{A_i} \quad (i = 1, 2), \quad (2.21)$$

where  $\gamma$  is a positive constant, and the potential difference between two pairs of

the supervision electrodes  $(M_1, M_2)$  and  $(N_1, N_2)$  is zero:

$$u|_{M_i} = u|_{N_i} \quad (i = 1, 2). \quad (2.22)$$

In the course of well-logging, the potential on the supervision electrodes  $(M_1, M_2)$  (or  $(N_1, N_2)$ ) is measured and denoted by  $U$ , with which we shall estimate the resistivity.

Since there are two pairs of screen electrodes and the second pair  $(A'_1, A'_2)$  has a big length, the main current  $I_0$  is almost perpendicular to the surface of the electrode  $A_0$  and penetrates deeply into the earth. This well-logging method is sensitive for the distant part of the formation.

Noting that the electrode system and the formation model possess the axis-symmetry and the symmetry about the middle plane of the formation, the potential is a function of variables  $r$  and  $z$ :  $u = u(r, z)$ , where  $r = \sqrt{x^2 + y^2}$  and the domain reduces to a 2-dimensional domain  $\Omega$  on the  $(r, z)$  plane shown in Fig. 2.3.

Thus, the quasi-harmonic equation (2.9) satisfied by the potential  $u$  changes its form into

$$-\frac{\partial}{\partial r}\left(\frac{r}{\rho}\frac{\partial u}{\partial r}\right) - \frac{\partial}{\partial z}\left(\frac{r}{\rho}\frac{\partial u}{\partial z}\right) = 0, \quad (2.23)$$

where  $\rho$  is defined by (2.3).

On each interface between the subdomains with different resistivity, the interface conditions (2.10) and (2.12) should be satisfied. On the surface of the earth  $z = Z$  and on the distant boundary  $r = R$ , we have  $u = 0$ . Denoting the union of these two parts of boundary by  $\Gamma_1$ , we have

$$u|_{\Gamma_1} = 0. \quad (2.24)$$

Denoting the union of the symmetric axis  $r = 0$ , the symmetric plane  $z = 0$  and all the insulation surfaces on the log-tool by  $\Gamma_2$ , we have

$$\left.\frac{r}{\rho}\frac{\partial u}{\partial n}\right|_{\Gamma_2} = 0. \quad (2.25)$$

Noticing the symmetry, on the upper half of the surface of the main electrode  $A_0$ , denoted by  $A_0/2$  which is located in the half plane  $z \geq 0$ , by (2.20) we have

$$\begin{cases} u = C_{A_0} \text{ (unknown constant),} \\ \int_{A_0/2} \frac{r}{\rho} \frac{\partial u}{\partial r} dz = \frac{I_0}{4\pi} \text{ (given constant).} \end{cases} \quad (2.26)$$

Similarly, on the supervision electrodes  $M_1$  and  $N_1$ , we have

$$\begin{cases} u = C_{M_1} \text{ (unknown constant),} \\ \int_{M_1} \frac{r}{\rho} \frac{\partial u}{\partial r} dz = 0, \end{cases} \quad (2.27)$$

$$\begin{cases} u = C_{N_1} \text{ (unknown constant),} \\ \int_{N_1} \frac{r}{\rho} \frac{\partial u}{\partial r} dz = 0 \end{cases} \quad (2.28)$$

respectively, and on the screen electrodes  $A_1$  and  $A'_1$  we have

$$\begin{cases} u = C_{A_1} \text{ (unknown constant),} \\ \int_{A_1} \frac{r}{\rho} \frac{\partial u}{\partial r} dz = \frac{I_1}{4\pi}, \end{cases} \quad (2.29)$$

$$\begin{cases} u = C_{A'_1} \text{ (unknown constant),} \\ \int_{A'_1} \frac{r}{\rho} \frac{\partial u}{\partial r} dz = \frac{I'_1}{4\pi} \end{cases} \quad (2.30)$$

respectively, where, by (2.21)-(2.22),  $I_1, I'_1$  are to be determined by the constraints

$$\begin{cases} u|_{A'_1} = \gamma u|_{A_1}, \\ u|_{M_1} = u|_{N_1}. \end{cases} \quad (2.31)$$

Since the problem is a linear one, we may take

$$I_0 = 1. \quad (2.32)$$

Let  $u_1(r, z)$  be the solution to boundary value problem (2.23)-(2.30), (2.10) and (2.12) with  $I_0 = 1$  and  $I_1 = I'_1 = 0$ ;  $u_2(r, z)$  the solution to the same boundary value problem with  $I_0 = 0, I_1 = 1$  and  $I'_1 = 0$ ; and  $u_3(r, z)$  the solution to the same boundary value problem with  $I_0 = I_1 = 0$  and  $I'_1 = 1$ . By linear superposition, the solution to the direct dual-lateral well-logging problem under consideration must be a linear combination of  $u_1, u_2$  and  $u_3$ :

$$u(r, z) = u_1(r, z) + \alpha u_2(r, z) + \beta u_3(r, z), \quad (2.33)$$

where constants  $\alpha, \beta$  are determined by (2.31), i.e.,

$$\begin{cases} u_1|_{A'_1} + \alpha u_2|_{A'_1} + \beta u_3|_{A'_1} = \gamma(u_1|_{A_1} + \alpha u_2|_{A_1} + \beta u_3|_{A_1}), \\ u_1|_{M_1} + \alpha u_2|_{M_1} + \beta u_3|_{M_1} = u_1|_{N_1} + \alpha u_2|_{N_1} + \beta u_3|_{N_1}. \end{cases} \quad (2.34)$$

### 2.3.2 Micro-spheric focusing well-logging

The micro-spheric focusing well-logging [5] is a very useful technique to detect the resistivity of the invaded zone. The electrode system is made of five concentric rectangular ring-shaped electrodes and a couple of return-circuit electrodes embedded into an insulation panel with the same curvature as the well-wall (see Fig. 2.5).

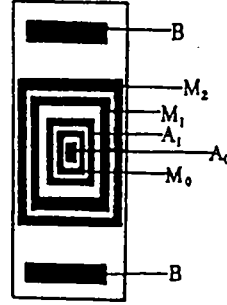


Figure 2.5

For the purpose of well-logging, the electrode panel is lowered into the drilled well and forced to contact the well-wall. The *main electrode*  $A_0$  discharges a static current  $I = I_0 + I_1$ , where  $I_0$ , called the *main current*, is the current absorbed by the return-circuite electrode  $B$ , while  $I_1$ , called the *auxiliary current*, is the current absorbed by the *auxiliary electrode*  $A_1$ . The instrument automatically adjusts  $I_0$  and  $I_1$  such that the potentials on the *supervision electrodes*  $M_1$  and  $M_2$  are equal to each other, i.e.,

$$u|_{M_1} - u|_{M_2} = 0 \quad (2.35)$$

and the potential difference between the *measuring electrode*  $M_0$  and the supervision electrode  $M_1$  (or  $M_2$ ) is a given constant  $V$ , i.e.,

$$u|_{M_0} - u|_{M_i} = V \quad (i = 1, 2). \quad (2.36)$$

Here, the main current  $I_0$  is measured.

In the present situation, even if the formation model is axi-symmetric, the problem can not be formulated into an axi-symmetric one, since the electrode contacts a part of the well-wall and a full 3-dimensional problem has to be considered. Noting the symmetry of the electrode system, the problem will be solved in the part  $x \geq 0, z \geq 0$  of the cylindrical domain  $\Omega : 0 \leq r \leq R, 0 \leq z \leq Z$ , shown in Fig.2.6.

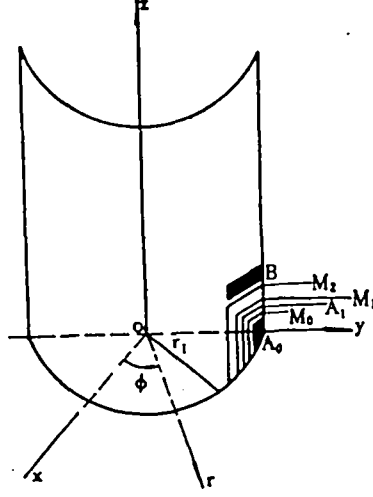


Figure 2.6

By (2.9), the potential function  $u = u(x, y, z)$  of the electric field satisfies

$$-\frac{\partial}{\partial x}\left(\frac{1}{\rho}\frac{\partial u}{\partial x}\right) - \frac{\partial}{\partial y}\left(\frac{1}{\rho}\frac{\partial u}{\partial y}\right) - \frac{\partial}{\partial z}\left(\frac{1}{\rho}\frac{\partial u}{\partial z}\right) = 0 \quad (2.37)$$

in each subdomain with constant resistivity, where  $\rho$  is defined by (2.4). On each interface, conditions (2.10) and (2.12) are satisfied. On  $r = R$  and  $z = Z$ , denoted by  $\Gamma_1$ , we have

$$u|_{\Gamma_1} = 0. \quad (2.38)$$

On the insulation surface and the symmetric boundary, denoted by  $\Gamma_2$ , we have

$$\left.\frac{1}{\rho}\frac{\partial u}{\partial n}\right|_{\Gamma_2} = 0. \quad (2.39)$$

On the main electrode  $A_0$ ,

$$\begin{cases} u|_{A_0} = C_{A_0} \text{ (unknown constant),} \\ \int \int_{A_0/4} \frac{1}{\rho} \frac{\partial u}{\partial n} dS = \frac{I_0 + I_1}{4}, \end{cases} \quad (2.40)$$

where  $A_0/4$  stands for the intersection of  $A_0$  and the boundary of  $\Omega$ . On the measuring electrode  $M_0$  and the supervision electrodes  $M_1, M_2$  we have

$$\begin{cases} u|_{M_i} = C_{M_i} \text{ (unknown constant),} \\ \int \int_{M_i/4} \frac{1}{\rho} \frac{\partial u}{\partial n} dS = 0, \end{cases} \quad (i = 0, 1, 2) \quad (2.41)$$

respectively. On the auxiliary electrode  $A_1$ ,

$$\begin{cases} u|_{A_1} = C_{A_1} \text{ (unknown constant),} \\ \int \int_{A_1/4} \frac{1}{\rho} \frac{\partial u}{\partial n} dS = -\frac{I_1}{4} \end{cases} \quad (2.42)$$

and on the return-circuit electrode B

$$\begin{cases} u|_B = C_B \text{ (unknown constant),} \\ \int \int_{B/4} \frac{1}{\rho} \frac{\partial u}{\partial n} dS = -\frac{I_0}{4}, \end{cases} \quad (2.43)$$

where  $I_0$  and  $I_1$  will be determined by (2.35)-(2.36).

Let  $u_i(x, y, z)$  ( $i = 1, 2$ ) be the solutions to boundary value problem (2.37)-(2.43), (2.10) and (2.12) with  $I_0 = 1, I_1 = 0$  and  $I_0 = 0, I_1 = 1$  respectively. The linear combination

$$u = u(x, y, z) = \alpha u_1(x, y, z) + \beta u_2(x, y, z) \quad (2.44)$$

is the solution to the direct problem for the micro spheric focusing well-logging, where  $\alpha, \beta$  are determined by (2.35)-(2.36), i.e.,

$$\begin{cases} \alpha(u_1|_{M_1} - u_1|_{M_2}) + \beta(u_2|_{M_1} - u_2|_{M_2}) = 0, \\ \alpha(u_1|_{M_0} - u_1|_{M_1}) + \beta(u_2|_{M_0} - u_2|_{M_1}) = V. \end{cases} \quad (2.45)$$

### 2.3.3 Inverse problem

If the coefficient  $\rho$  is not completely known, but some additional information about the potential  $u$  is given, to solve simutaniously the coefficient  $\rho$  and the potential  $u$  provides one kind of inverse problem. Since  $\rho$  is piecewise constant, this kind of inverse problem reduces to a parameter identification problem to identify some resistivity parameters ( $R_t, R_{xo}, R_s$ , etc.) and some geometric parameters (thickness of the objective formation, depth of the invaded zone, etc.). In what follows we shall first consider the direct problem.

## 3 Variational principle, existence and uniqueness of the solution

The direct problem for the resistivity well-logging asks us to solve the following problem:

$$-\nabla\left(\frac{1}{\rho}\nabla u\right) = 0 \quad (3.1)$$

in each subdomain of  $\Omega$  with constant  $\rho$ ; On each interface between the subdomains with different resistivity:

$$\begin{cases} u_- = u_+, \\ (\frac{1}{\rho} \frac{\partial u}{\partial n})_- = (\frac{1}{\rho} \frac{\partial u}{\partial n})_+; \end{cases} \quad (3.2)$$

$$u|_{\Gamma_1} = 0; \quad (3.3)$$

$$\frac{1}{\rho} \frac{\partial u}{\partial n} |_{\Gamma_2} = 0; \quad (3.4)$$

On the surface of each electrode  $\Gamma_0^i$  ( $i = 1, 2, \dots, L$ ),

$$\begin{cases} u = C_i \text{ (unknown constant),} \\ \int_{\Gamma_0^i} \frac{1}{\rho} \frac{\partial u}{\partial n} dS = I_i \text{ (given constant).} \end{cases} \quad (3.5)$$

Here  $\Gamma$ , the boundary of  $\Omega$ , is the union of  $\Gamma_1$ ,  $\Gamma_2$  and  $\Gamma_0^i$  ( $i = 1, 2, \dots, L$ ) which do not overlap each other and  $\overline{\Gamma_0^i} \cap \overline{\Gamma_1} = \emptyset$ ,  $\overline{\Gamma_0^i} \cap \overline{\Gamma_0^j} = \emptyset$  ( $i \neq j; i, j = 1, \dots, L$ ); moreover,  $\rho \geq \alpha_0 > 0$ , where  $\alpha_0$  is a constant.

Introduce the following closed subspace of  $H^1(\Omega)$ :

$$V_0 = \{v = v(x, y, z) \mid v \in H^1(\Omega), v|_{\Gamma_1} = 0, v|_{\Gamma_0^i} = \text{const}(i = 1, \dots, L)\}. \quad (3.6)$$

$u$  is called to be a weak solution to boundary value problem (3.1)-(3.5), if  $u \in V_0$  such that

$$a(u, \phi) = L(\phi), \quad \forall \phi \in V_0, \quad (3.7)$$

or, equivalently, if  $u \in V_0$  such that

$$J(u) = \min_{v \in V_0} J(v), \quad (3.8)$$

where

$$a(u, \phi) = \int \int \int_{\Omega} \frac{1}{\rho} \nabla u \nabla \phi \, dx dy dz, \quad (3.9)$$

$$L(\phi) = \sum_{i=1}^L I_i \phi|_{\Gamma_0^i} \quad (3.10)$$

and

$$J(v) = \frac{1}{2} a(v, v) - L(v). \quad (3.11)$$

By Lax-Milgram theorem, it is easy to show that problem (3.1)-(3.5) admits a unique weak solution  $u \in V_0$  [3-4].

## 4 Numerical solution by the finite element method

Due to the variational principle in section 3, solving the boundary value problem related to the resistivity well-logging is equivalent to find the minimum of the functional

$$J(v) = \frac{1}{2} \int \int \int_{\Omega} \frac{1}{\rho} |\nabla v|^2 dx dy dz - \sum_{i=1}^L I_i v|_{\Gamma_i^0} \quad (4.1)$$

on the space

$$V_0 = \{v = v(x, y, z) \mid v \in H^1(\Omega), v|_{\Gamma_1} = 0, v|_{\Gamma_i^0} = \text{const} \ (i = 1, \dots, L)\}, \quad (4.2)$$

i.e., to find  $u \in V_0$  such that

$$J(u) = \min_{v \in V_0} J(v), \quad (4.3)$$

which is equivalent to find  $u \in V_0$  such that

$$\int \int \int_{\Omega} \frac{1}{\rho} \nabla u \nabla \phi dx dy dz = \sum_{i=1}^L I_i \phi|_{\Gamma_i^0}, \quad \forall \phi \in V_0, \quad (4.4)$$

where  $\Gamma_i^0$  stands for the surface of the  $i$ -th electrode and  $I_i$  is the current discharged by it ( $i = 1, \dots, L$ ).

Problem (4.3) or (4.4) can be numerically solved by Ritz or Galerkin finite element method [5-6]. Nevertheless some special skills have to be used to treat the total flux boundary condition.

### 4.1 Stiffness matrix

We can form the stiffness matrix by the standard procedure of the finite element method, then treat the total flux boundary condition. We now use some geometric quantities to represent the finite element equations, as an example, for the dual-lateral well-logging.



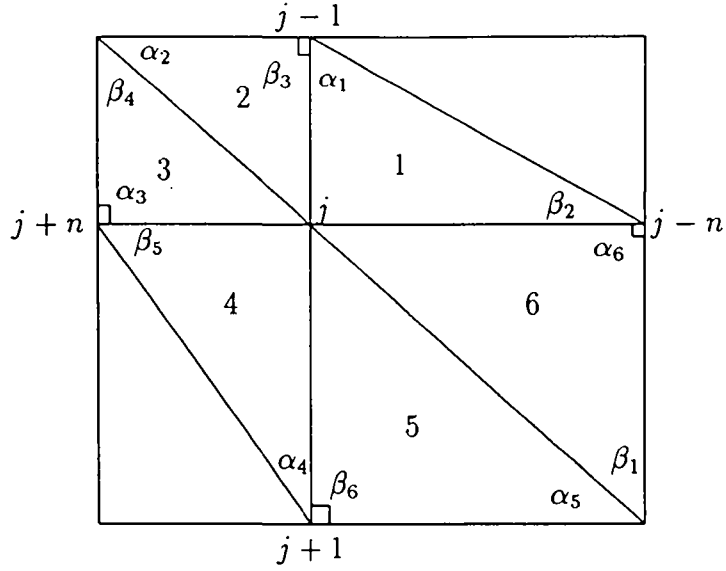


Figure 4.1

Since the problem is axi-symmetric, we can take a 2-dimensional partition on the domain  $\Omega$  in the  $(r, z)$  plane (cf. Figure 2.3). We use the linear triangle element based on the perpendicular network. Suppose that there are  $n$  nodepoints on each net-line parallel to the well-axis and the total number of the nodepoints is  $N$ . If the  $j$ -th node is an interior node shown in Fig.4.1, the  $j$ -th row of the stiffness matrix is (see [7])

$$[0, \dots, 0, k_{j,j-n}, 0, \dots, 0, k_{j,j-1}, k_{j,j}, k_{j,j+1}, 0, \dots, 0, k_{j,j+n}, 0, \dots, 0], \quad (4.5)$$

where

$$\begin{cases} k_{j,j-n} = -(\frac{\bar{r}_1}{2R_I} \cot \alpha_1 + \frac{\bar{r}_6}{2R_{IV}} \cot \beta_1), \\ k_{j,j-1} = -(\frac{\bar{r}_2}{2R_{II}} \cot \alpha_2 + \frac{\bar{r}_1}{2R_I} \cot \beta_2), \\ k_{j,j+1} = -(\frac{\bar{r}_5}{2R_{IV}} \cot \alpha_5 + \frac{\bar{r}_4}{2R_{III}} \cot \beta_5), \\ k_{j,j+n} = -(\frac{\bar{r}_4}{2R_{III}} \cot \alpha_4 + \frac{\bar{r}_3}{2R_{II}} \cot \beta_4), \\ k_{j,j} = -(k_{j,j-n} + k_{j,j-1} + k_{j,j+1} + k_{j,j+n}), \end{cases} \quad (4.6)$$

and  $\bar{r}_i$  is the  $r$ -coordinate of the gravity center for the  $i$ -th triangle element around the node  $j$  ( $i = 1, \dots, 6$ );  $R_I, R_{II}, R_{III}, R_{IV}$  denote the resistivities in four quadrants around  $j$  respectively;  $\alpha_i, \beta_i$  ( $i = 1, \dots, 6$ ) are the inner angles of elements shown in Fig.4.1.

Similarly we can form the corresponding row of the stiffness matrix for each boundary node.

Thus, we obtain the stiffness matrix

$$K = (k_{s,t})_{N \times N}. \quad (4.7)$$

## 4.2 Treatment for equi-valued surfaces

Before solving the finite element equations, we have to consider the constraints on the equi-valued surfaces. Without loss of generality, we suppose that there is only one equi-valued surface  $\Gamma_0$  (electrode) with nodepoints numbered by  $l, l+1, \dots, m-1, m$ . Moreover, for simplicity of statement we suppose that  $\Gamma_1 = \emptyset$ . Let the unknown vector of the node potential be

$$\delta = (u_1, u_2, \dots, u_N)^T. \quad (4.8)$$

There should be

$$u_l = u_{l+1} = \dots = u_{m-1} = u_m. \quad (4.9)$$

Taking the following invertible transformation

$$\begin{cases} v_l = u_l - u_{l+1}, \\ v_{l+1} = u_{l+1} - u_{l+2}, \\ \vdots \\ v_{m-1} = u_{m-1} - u_m, \\ v_m = u_m, \end{cases} \quad (4.10)$$

we have

$$v_l = v_{l+1} = \dots = v_{m-1} = 0. \quad (4.11)$$

The inverse transformation of (4.10) is

$$\begin{cases} u_l = v_l + v_{l+1} + \dots + v_{m-1} + v_m, \\ u_{l+1} = v_{l+1} + \dots + v_m, \\ \vdots \\ u_{m-1} = v_{m-1} + v_m, \\ u_m = v_m. \end{cases} \quad (4.12)$$

The quadratic form

$$J = \frac{1}{2} \delta^T K \delta - \frac{I}{4\pi} u|_{\Gamma_0}, \quad (4.13)$$

which is a discrete form of the quadratic functionnal

$$J(u) = \frac{1}{2} \int \int_{\Omega} \frac{r}{\rho} |\nabla u|^2 dr dz - \frac{I}{4\pi} u|_{\Gamma_0}, \quad (4.14)$$

should be changed relevantly.

Let

$$\delta_A = (u_l, u_{l+1}, \dots, u_{m-1}, u_m)^T, \quad (4.15)$$

$$\tilde{\delta}_A = (v_l, v_{l+1}, \dots, v_{m-1}, v_m)^T \quad (4.16)$$

and

$$\delta = \begin{bmatrix} \delta_1 \\ \delta_A \\ \delta_2 \end{bmatrix}, \quad \tilde{\delta} = \begin{bmatrix} \delta_1 \\ \tilde{\delta}_A \\ \delta_2 \end{bmatrix}, \quad (4.17)$$

where

$$\delta_1 = (u_1, \dots, u_{l-1})^T, \quad (4.18)$$

$$\delta_2 = (u_{m+1}, \dots, u_N)^T. \quad (4.19)$$

Setting

$$R_A = \begin{bmatrix} 1 & 1 & \dots & 1 \\ & 1 & \dots & 1 \\ O & & \ddots & \\ & & & 1 \end{bmatrix}, \quad (4.20)$$

which is an  $(m-l+1) \times (m-l+1)$  upper triangular matrix, by (4.12) we have

$$\delta_A = R_A \tilde{\delta}_A. \quad (4.21)$$

Therefore

$$\delta = R \tilde{\delta} \quad (4.22)$$

with

$$R = \begin{bmatrix} E_1 & 0 & 0 \\ 0 & R_A & 0 \\ 0 & 0 & E_2 \end{bmatrix}, \quad (4.23)$$

where  $E_1$  is the unit matrix of order  $(l-1)$  and  $E_2$  is the unit matrix of order  $(N-m)$ . Thus, the quadratic form (4.13) turns into

$$\begin{aligned} J &= \frac{1}{2} \delta^T K \delta - \frac{I}{4\pi} u_m \\ &= \frac{1}{2} \tilde{\delta}^T \tilde{K} \tilde{\delta} - \frac{I}{4\pi} v_m, \end{aligned} \quad (4.24)$$

where

$$\tilde{K} = R^T K R. \quad (4.25)$$

Let

$$\tilde{\delta} = (u_1, \dots, u_{l-1}, u_m, \dots, u_L)^T \quad (4.26)$$

and let  $\tilde{\tilde{K}}$  be the submatrix of  $\tilde{K}$ , obtained by deleting the rows and the columns corresponding to the indices from  $l$  to  $m-1$ . Noticing (4.11) we have

$$J = \frac{1}{2} \tilde{\delta}^T \tilde{\tilde{K}} \tilde{\delta} - \tilde{\delta}^T \tilde{P}, \quad (4.27)$$

where

$$\tilde{P} = (0, \dots, 0, \frac{I}{4\pi}, 0, \dots, 0)^T. \quad (4.28)$$

If  $K$  is written as

$$\begin{bmatrix} K_1 & & \text{sym.} \\ K_A^* & K_A & \\ K_3 & K_A^{**} & K_2 \end{bmatrix}, \quad (4.29)$$

we have

$$\tilde{\tilde{K}} = \begin{bmatrix} K_1 & & \text{sym.} \\ \overline{K}_A^* & \overline{k}_{ll} & \\ K_3 & \overline{K}_A^{**} & K_2 \end{bmatrix} \quad (4.30)$$

with

$$\overline{K}_A^* = (\sum_{j=l}^m k_{j1}, \sum_{j=l}^m k_{j2}, \dots, \sum_{j=l}^m k_{j,l-1}), \quad (4.31)$$

$$\overline{k}_{ll} = \sum_{i=l}^m \sum_{j=l}^m k_{ij} \quad (4.32)$$

and

$$\overline{K}_A^{**} = (\sum_{j=l}^m k_{m+1,j}, \sum_{j=l}^m k_{m+2,j}, \dots, \sum_{j=l}^m k_{N,j})^T. \quad (4.33)$$

Thus we finish the treatment on the equi-valued surface and get the system of finite element equations

$$\tilde{\tilde{K}} \tilde{\delta} = \tilde{P}, \quad (4.34)$$

where  $\tilde{P}$  is given by (4.28).

### 4.3 Remarks

The problem for the micro-spheric focusing well-logging is a full 3-dimensional problem. Noting the symmetry, it is convenient to make the finite element partition on a cuboid

$$\begin{cases} r_b \leq r \leq R, \\ -\frac{\pi}{2} \leq \phi \leq \frac{\pi}{2}, \\ 0 \leq z \leq Z \end{cases} \quad (4.35)$$

in the cylindrical coordinates  $(r, \phi, z)$ , where  $r_b$  is equal to the difference between the well-radius and the thickness of the mud-cake. First of all, we divide  $(r_b, R)$  into  $H$  parts by points  $r_i (i = 0, \dots, H)$  with  $r_0 = r_b, r_H = R$  and  $r_i < r_{i+1}$  ( $i = 0, \dots, H - 1$ ). We can take  $\Delta r_i = (r_{i+1} - r_i)$  to be increasing with respect to  $i = 0, \dots, H - 1$ .

We can use the same 2-dimensional element partition as in §4.1 for each plane domain  $r = r_i, -\frac{\pi}{2} \leq \phi \leq \frac{\pi}{2}, 0 \leq z \leq Z$  ( $i = 0, \dots, H$ ), and by connecting the corresponding nodes on neighbouring planes, we get a 3-dimensional element partition. Since all the 2-dimensional elements are triangles, we get a 3-dimensional mesh with triangular prisms.

By similarity of the elements, we can devise an algorithm to form the stiffness matrix very quickly.

In the numerical simulation, usually we only need the values of the potential on the electrodes. It is beneficial to number the node points on electrodes at the last, so that only a few last unknowns have to be solved.

It is easy to see that the following similarity property holds: the solution  $u = u(x, y, z)$  corresponding to the resistivity  $\rho$  will change into  $\bar{u} = \alpha u(x, y, z)$ , if the resistivity  $\rho$  changes into  $\alpha \rho$ , where  $\alpha$  is an arbitrary positive number. Then, in the numerical simulation we may fix the resistivity in one subdomain, say, in  $R_{xo}$ , to be equal to 1 and take the resistivity in other subdomains to be  $R_s/R_{xo}, R_t/R_{xo}$ , etc.

While we make interpretation chart for the well-logging or interpret the well-logging information by the computer, we have to do a great amount of calculation for various formation resistivities. For example, in the micro-spheric focusing well-logging, if we separate  $R_{xo}$  and  $R_{mc}$  into  $n$  levels, we need to solve the problem  $n^2$  times. Nevertheless, by similarity, only  $n$  times are enough.

Besides, since the resistivity in the invaded zone is always supposed to be 1, the resistivity distribution turns into

$$\bar{\rho} = \begin{cases} R_{mc}/R_{xo}, & r_b < r < r_2, \\ 1, & r_2 < r < R, \end{cases} \quad (4.36)$$

where  $r_2$  is the well-radius. Thus, when a direct technique is used to solve the system of finite element equations, the equations for the interior nodes in the invaded zone only need to be formed and decomposed once for all different values of  $R_{mc}/R_{xo}$ . Thus, what we have to do for each concrete value of  $R_{mc}/R_{xo}$  is to form the equations for other nodes and make the corresponding decomposition to obtain the solution. In such a way much computation time is saved.

## 5 Numerical results

By use of the mathematical model given by the total flux boundary value problem, the numerical simulation by the finite element method produces very accurate results [5], [8].

In the well-logging interpretation there are two important parameters: the instrument constant  $K_0$  and the apparent resistivity  $\rho_A$ . For the micro-spheric focusing well-logging,

$$K_0 = \frac{\tilde{I}_0}{V} \quad (5.1)$$

and

$$\rho_A \triangleq R_{MSFL} = K_0 \cdot \frac{V}{I_0}, \quad (5.2)$$

where  $\tilde{I}_0$  is the main current obtained in the homogeneous case  $\rho = 1$ ,  $I_0$  is the main current, and  $V$  is given by (2.36).

For a given electrode panel, we use our model to do the numerical simulation and obtain the instrument constant  $K_0 = 0.0976$ . In the meantime, by using a physical experiment to determine the same instrument constant, we obtain  $K_0 = 0.0988$ . The relative error is only 1.21%.

For the mud-cake thicknesses 5, 10, 15, 20, 25, 30 (*mm*) and  $R_{xo}/R_{mc}$  values 2, 5, 10, 50, 100, we do the computation and draw the characterizing curve shown in Fig. 5.1. To interpret the well-logging information, for different mud-cake thicknesses and different values of  $R_{xo}/R_{mc}$  we draw the resulting curves with the auxiliary current ratio  $\eta = I_1/I_0$  or  $\eta \cdot (R_{mc}/1.91R_{MSFL})$  as the horizontal coordinate and  $R_{MSFL}/R_{mc}$  as the vertical coordinate (see Fig.5.2 and Fig.5.3). These charts have been successfully used to interpret the well-logging information in practical exploitation for many oil fields in China.

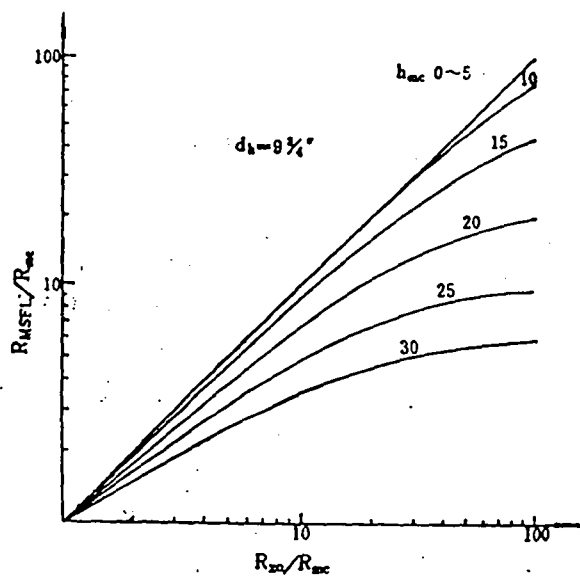


Figure 5.1

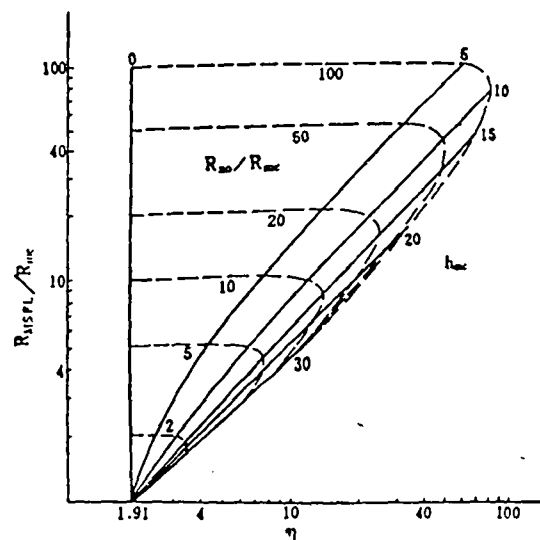


Figure 5.2

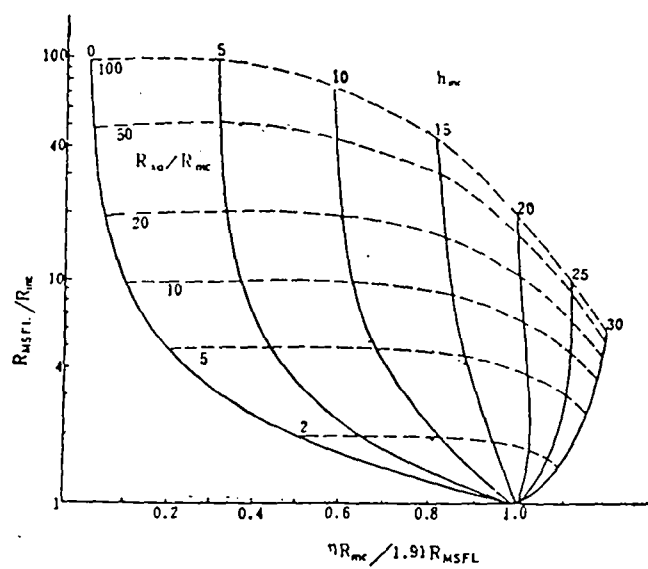


Figure 5.3

## 6 Connection between the total flux boundary value problem and the classical boundary value problems

The resistivity well-logging problem can be also formulated by the classical boundary value problem instead of by the total flux boundary value problem. Nevertheless this way usually loses the accuracy, and takes more computing time since more boundary value problems must be solved.

For example, the micro-spheric focusing well-logging problem has been formulated to a couple of total flux boundary value problems given in Section 2.3.2. But the same problem must be formulated by five classical boundary value problems as follows:

Let  $u_1, u_2, u_3, u_4$  and  $u_5$  be the solutions to the following classical boundary value problems respectively:

$$\left\{ \begin{array}{l} (2.37)-(2.39), (2.10), (2.12), \\ u|_{A_0} = 1, \\ u|_{A_1} = 0, \\ u|_B = 0, \\ u|_{M_1} = u|_{M_2} = 0, \\ u|_{M_0} = 0; \end{array} \right. \quad (6.1)$$

$$\left\{ \begin{array}{l} (2.37)-(2.39), (2.10), (2.12), \\ u|_{A_0} = 0, \\ u|_{A_1} = 1, \\ u|_B = 0, \\ u|_{M_1} = u|_{M_2} = 0, \\ u|_{M_0} = 0; \end{array} \right. \quad (6.2)$$

$$\left\{ \begin{array}{l} (2.37)-(2.39), (2.10), (2.12), \\ u|_{A_0} = 0, \\ u|_{A_1} = 0, \\ u|_B = 1, \\ u|_{M_1} = u|_{M_2} = 0, \\ u|_{M_0} = 0; \end{array} \right. \quad (6.3)$$

$$\left\{ \begin{array}{l} (2.37)-(2.39), (2.10), (2.12), \\ u|_{A_0} = 0, \\ u|_{A_1} = 0, \\ u|_B = 0, \\ u|_{M_1} = u|_{M_2} = 1, \\ u|_{M_0} = 0; \end{array} \right. \quad (6.4)$$



$$\left\{ \begin{array}{l} (2.37)-(2.39), (2.10), (2.12), \\ u|_{A_0} = 0, \\ u|_{A_1} = 0, \\ u|_B = 0, \\ u|_{M_1} = u|_{M_2} = 0, \\ u|_{M_0} = 1. \end{array} \right. \quad (6.5)$$

The solution to the micro-spheric focusing well-logging problem should be the linear combination of  $u_1, u_2, u_3, u_4$  and  $u_5$ :

$$u = a_1 u_1 + a_2 u_2 + a_3 u_3 + a_4 u_4 + a_5 u_5, \quad (6.6)$$

where  $a_i (i = 1, \dots, 5)$  are determined by

$$\left\{ \begin{array}{l} u|_{M_0} - u|_{M_1} = V, \\ \int \int_{M_0} \frac{1}{\rho} \frac{\partial u}{\partial n} dS = 0, \\ \int \int_{M_1+M_2} \frac{1}{\rho} \frac{\partial u}{\partial n} dS = 0, \\ \int \int_{A_0} \frac{1}{\rho} \frac{\partial u}{\partial n} dS = I, \\ \int \int_{A_1+B} \frac{1}{\rho} \frac{\partial u}{\partial n} dS = -I. \end{array} \right. \quad (6.7)$$

Moreover, for solving  $a_i (i = 1, \dots, 5)$  we have to use the numerical derivation and numerical integration in (6.7), hence the numerical error would be amplified.

Therefore, formulating the well-logging problem by the classical boundary value problem is a less economical and less accurate way. Thus, using the total flux boundary value problem is the best way to model the resistivity well-logging problem.

Wei [11] and Sun [10] investigated the limiting behaviour while the size of an electrode that charges no current tends to zero. They concluded that the solution to the total flux boundary value problem converges to the solution to the boundary value problem without that electrode. It means that when the total flux is zero, if the size of the electrode is relatively small we may omit the total flux boundary condition, i.e., the total flux boundary condition can be replaced by the classical Neumann boundary condition  $\frac{\partial u}{\partial n} = 0$ .

## 7 Electrode homogenization

In some well-loggings, e.g., the micro-lateral well-logging and the micro-spheric focusing well-logging, the aim is to detect the resistivity in the area near the well-

bore. The electrodes are lowered into the drilled well and forced to snugly fit the well-wall. For this purpose, the engineers have designed the patched electrode  $\Gamma_0$  which is made of many electrode cells linked by wire on a rubber plate, as shown in Fig.7.1. In this case the boundary condition on  $\Gamma_0$  changes into the mixture of two parts: On the surface of the rubber

$$\frac{1}{\rho} \frac{\partial u}{\partial n} = 0; \quad (7.1)$$

while on the union of the metal cells of electrode:

$$u = C \text{ is an unknown constant} \quad (7.2)$$

and the total flux

$$\int \int \frac{1}{\rho} \frac{\partial u}{\partial n} dS \text{ is a given quantity } I. \quad (7.3)$$

When the size of electrode cell is very small and then the number of electrode cells is large enough, the boundary condition on  $\Gamma_0$  becomes so complicated that even if a very meticulous mesh is used, we can not get a good numerical solution by the finite element method.

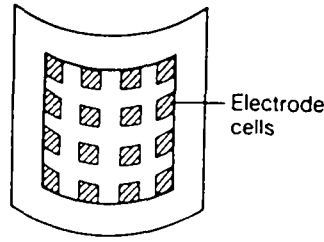


Figure 7.1

The boundary homogenization technique suggested by A.Damlamian and Li Ta-tsien [12-13] and Li Ta-tsien [14] can be used to simplify this kind of boundary condition on  $\Gamma_0$  and to reduce the complexity efficiently.

Without loss of generality, we only discuss the case with a single patched electrode. Suppose that  $\Omega$  is a domain in  $R^3$  with boundary  $\Gamma$  which is separated into three parts  $\Gamma_1, \Gamma_2$  and  $\Gamma_0$ , where  $\Gamma_1$  and  $\Gamma_2$  are defined as before, while  $\Gamma_0$  stands for the patched electrode.

Thus, the surface  $\Gamma_0$  is divided into two regular subsets  $\Gamma_0^\varepsilon$  and  $\tilde{\Gamma}_0^\varepsilon$ , where  $\tilde{\Gamma}_0^\varepsilon$  is composed of insulation material, while  $\Gamma_0^\varepsilon$ , the surface of piecewise electrodes, is composed of a number of connected surfaces  $\Gamma_{0,i}^\varepsilon (i = 1, \dots, m(\varepsilon))$ :

$$\Gamma_0^\varepsilon = \bigcup_{i=1}^{m(\varepsilon)} \Gamma_{0,i}^\varepsilon, \quad (7.4)$$

in which each  $\Gamma_{0,i}^\epsilon$  denotes the surface of a connected piece of electrode. Since these connected pieces are linked each other by wire, the potential  $u$  must be constant on the whole  $\Gamma_0^\epsilon$ . On the other hand, the total current discharged from  $\Gamma_0^\epsilon$  is still the given constant  $I$ .

The boundary value problem corresponding to the case of patched electrode is

$$\begin{cases} -\nabla \left( \frac{1}{\rho} \nabla u_\epsilon \right) = 0 & \text{in } \Omega \text{ except the interfaces,} \\ u_\epsilon \text{ satisfies (2.10) and (2.12) on each interface,} \\ u_\epsilon|_{\Gamma_1} = 0, \quad \frac{\partial u_\epsilon}{\partial n}\bigg|_{\Gamma_2} = 0, \\ \frac{\partial u_\epsilon}{\partial n}\bigg|_{\tilde{\Gamma}_0^\epsilon} = 0, \\ u_\epsilon|_{\Gamma_0^\epsilon} = C_\epsilon \text{ (unknown constant),} \quad \int_{\Gamma_0^\epsilon} \frac{1}{\rho} \frac{\partial u}{\partial n} dS = I. \end{cases} \quad (7.5)$$

Let

$$\chi_\epsilon = \begin{cases} 1 & \text{on } \Gamma_{0,i}^\epsilon, \\ 0 & \text{on } \tilde{\Gamma}_0^\epsilon \end{cases} \quad (7.6)$$

be the characteristic function of  $\Gamma_0^\epsilon$  on  $\Gamma_0$ . We make the following hypothesis:

(H) For any weak \* convergent subsequence  $\{\chi_{\epsilon'}\}$  of  $\{\chi_\epsilon\}$  in  $L^\infty(\Gamma_0)$ , its limit function is always different from zero almost everywhere on  $\Gamma_0$ ; namely, if

$$\chi_{\epsilon'} \rightharpoonup \chi \text{ weak } * \text{ in } L^\infty(\Gamma_0), \quad (7.7)$$

then

$$\chi \neq 0 \text{ a.e. on } \Gamma_0. \quad (7.8)$$

Hypothesis (H) actually gives a restriction on the geometric structure of  $\Gamma_0^\epsilon$  as  $\epsilon \rightarrow 0$ . In fact, it follows from (H) that there exists a constant  $a > 0$  such that for any fixed  $\epsilon > 0$

$$\text{meas}_{\Gamma_0} \Gamma_0^\epsilon \geq a > 0. \quad (7.9)$$

Particularly, in the case of periodic structure as shown in Fig.7.2, the whole sequence

$$\chi_\epsilon \rightharpoonup \theta \neq 0 \text{ weak } * \text{ in } L^\infty(\Gamma_0) \quad \text{as } \epsilon \rightarrow 0, \quad (7.10)$$

so that (H) is automatically satisfied.

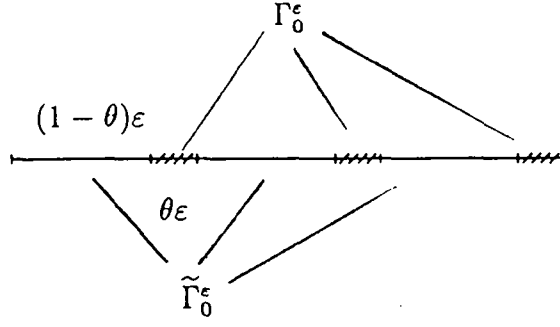


Figure 7.2

Introducing the space

$$V_\epsilon = \{\phi \in H^1(\Omega) \mid \phi|_{\Gamma_1} = 0, \phi|_{\Gamma_0^\epsilon} = \text{const}\}, \quad (7.11)$$

the solution  $u_\epsilon \in V_\epsilon$  to problem (7.5) is characterized by

$$\int \int \int_\Omega \frac{1}{\rho} \nabla u_\epsilon \nabla \phi \, dx dy dz = I \phi|_{\Gamma_0^\epsilon}, \quad \forall \phi \in V_\epsilon. \quad (7.12)$$

Taking  $\phi = u_\epsilon$  in (7.12), we obtain

$$\int \int \int_\Omega \frac{1}{\rho} |\nabla u_\epsilon|^2 \, dx dy dz = I u_\epsilon|_{\Gamma_0^\epsilon}. \quad (7.13)$$

Then, due to Poincaré inequality and the trace theorem, it is no difficult to see that  $u_\epsilon$  is bounded in  $H^1(\Omega)$  and  $C_\epsilon = u_\epsilon|_{\Gamma_0^\epsilon}$  is bounded. By extracting a proper subsequence  $\epsilon_n$  tending to zero, we conclude that there exists  $u \in H^1(\Omega)$  such that

$$u_{\epsilon_n} \rightharpoonup u \text{ weakly in } H^1(\Omega). \quad (7.14)$$

Taking  $\epsilon_n \rightarrow 0$  on both sides of  $u_{\epsilon_n} \chi_{\epsilon_n} = C_{\epsilon_n} \chi_{\epsilon_n}$ , we get  $u|_{\Gamma_0} \cdot \chi = C \chi$ , where  $C$  is the limit of the sequence  $C_{\epsilon_n}$ . Consequently, from hypothesis (H) we have

$$u|_{\Gamma_0} = C. \quad (7.15)$$

Introduce the space

$$V = \{\phi \in H^1(\Omega) \mid \phi|_{\Gamma_1} = 0, \phi|_{\Gamma_0} = \text{const}\}. \quad (7.16)$$

It is clear that  $V \subset V_\epsilon$  and  $u \in V$ . Therefore, from (7.12) we obtain

$$\int \int \int_\Omega \frac{1}{\rho} \nabla u_\epsilon \nabla \phi \, dx dy dz = I \phi|_{\Gamma_0}, \quad \forall \phi \in V. \quad (7.17)$$

Then, choosing  $\varepsilon = \varepsilon_n$  and taking the limit, we obtain

$$\int \int \int_{\Omega} \frac{1}{\rho} \nabla u \nabla \phi \, dx dy dz = I \phi|_{\Gamma_0}, \quad \forall \phi \in V. \quad (7.18)$$

This is nothing but the variational formula for the following problem:

$$\begin{cases} -\nabla \left( \frac{1}{\rho} \nabla u \right) = 0 & \text{in } \Omega \text{ except the interfaces,} \\ u \text{ satisfies (2.10) and (2.12) on each interface,} \\ u|_{\Gamma_1} = 0, \quad \frac{\partial u}{\partial n} \Big|_{\Gamma_2} = 0, \\ u|_{\Gamma_0} = C \text{ (unknown constant),} \quad \int \int_{\Gamma_0} \frac{1}{\rho} \frac{\partial u}{\partial n} dS = I. \end{cases} \quad (7.19)$$

- So  $u$ , the limit of  $u_{\varepsilon_n}$ , is the solution to problem (7.19). From the uniqueness of the solution to problem (7.19), the whole sequence  $u_{\varepsilon}$  converges to  $u$  as  $\varepsilon \rightarrow 0$ . Noticing that by (7.13) and (7.18), the  $H^1(\Omega)$  norm of  $u_{\varepsilon}$  converges to the  $H^1(\Omega)$  norm of  $u$ , we conclude that  $u_{\varepsilon}$  converges to  $u$ , strongly in  $H^1(\Omega)$ .

Thus, the homogenized boundary condition on  $\Gamma_0$  is the following total flux boundary condition:

$$\begin{cases} u|_{\Gamma_0} = C \text{ (unknown constant),} \\ \int \int_{\Gamma_0} \frac{1}{\rho} \frac{\partial u}{\partial n} dS = I. \end{cases} \quad (7.20)$$

Hence, in the problem of resistivity well-logging, if the size of each connected piece of patched electrode is relatively small, instead of the patched electrode we can approximately regard the whole surface  $\Gamma_0$  as an electrode and the complexity is then reduced.

## 8 Inverse problems

The main purpose of resistivity well-logging is to determine the formation resistivity by measuring some information from the well-logging field, in other words, to determine certain coefficients in the partial differential equation by some additional information of the solution to the corresponding boundary value problem. The author of [15] proved the uniqueness of the solution to the inverse problem to determine the near constant coefficient in a quasiharmonic equation, provided that both the potential and the flux on the whole boundary are measured. Nevertheless, in the case of well-logging, it is very difficult to measure the potential and the flux on the whole boundary. As mentioned above, by the assumption of oil-geophysics, the coefficient of the equation is simplified to be piecewise constant, so the inverse problem turns into a parameter identification problem, in

which several physical parameters (resistivities in different formations) and several geometric parameters (depth of the invaded zone, thickness of the objective layer etc.) are to be determined.

Tan [16], Li & Tan [17] obtained the well-posedness for the case of identifying a single physical or geometric parameter.

First of all, we illustrate how to identify the depth of the invaded zone. This is an identification problem for a single geometric parameter. For simplicity and without loss of generality, we suppose that the domain  $\Omega$  is only composed of two subdomains  $\Omega_{xo}$  and  $\Omega_t$  and there is only one electrode. Let  $h$  be the depth of the invaded zone. We denote

$$\begin{cases} \Omega_h = \Omega_{xo}, \\ \Omega_{H-h} = \Omega_t, \end{cases} \quad (8.1)$$

as shown in Fig.8.1, and then we have

$$\rho = \begin{cases} R_{xo} & \text{in } \Omega_h, \\ R_t & \text{in } \Omega_{H-h}. \end{cases} \quad (8.2)$$

Since the water increases the conductivity of the formation, we always have

$$R_{xo} < R_t. \quad (8.3)$$

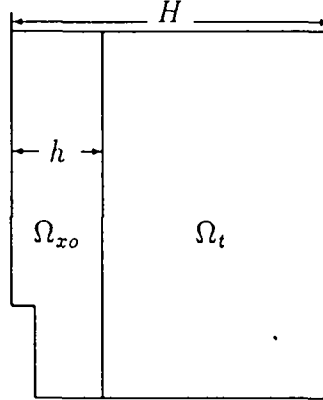


Figure 8.1

Now suppose that the piecewise constant resistivity and all the geometric parameters except  $h$ , the depth of the invaded zone, are known, we investigate the following identification problem  $(P_h)$ : To find  $(h, u_h(x, y)) \in [0, H] \times H^1(\Omega)$

such that

$$\begin{cases} -\frac{\partial}{\partial x}(\frac{1}{\rho} \frac{\partial u_h}{\partial x}) - \frac{\partial}{\partial y}(\frac{1}{\rho} \frac{\partial u_h}{\partial y}) - \frac{\partial}{\partial z}(\frac{1}{\rho} \frac{\partial u_h}{\partial z}) = 0 & \text{in } \Omega_h \cup \Omega_{H-h}, \\ u_h \text{ satisfies (2.10) and (2.12) on the interface between } \Omega_h \text{ and } \Omega_{H-h}, \\ u_h|_{\Gamma_1} = 0, \quad \frac{\partial u_h}{\partial n}\bigg|_{\Gamma_2} = 0, \\ u_h|_{\Gamma_0} = \bar{U}, \quad \int_{\Gamma_0} \frac{1}{\rho} \frac{\partial u_h}{\partial n} dS = I, \end{cases} \quad (8.4)$$

where both  $\bar{U}$  and  $I$  are all given constants and  $\rho$  is defined by (8.2).

Let

$$V = \{v \in H^1(\Omega) \mid v|_{\Gamma_1} = 0, v|_{\Gamma_0} = \text{const}\} \quad (8.5)$$

and

$$J_h(v) = \frac{1}{2} \int \int \int_{\Omega_h} \frac{1}{R_{x_0}} |\nabla v|^2 dx dy dz + \frac{1}{2} \int \int \int_{\Omega_{H-h}} \frac{1}{R_t} |\nabla v|^2 dx dy dz - Iv|_{\Gamma_0}. \quad (8.6)$$

For any fixed  $h \in [0, H]$ , there exists a unique  $u_h \in V$  such that

$$J_h(u_h) = \min_{v \in V} J_h(v), \quad (8.7)$$

and  $u_h$  is characterized by

$$\int \int \int_{\Omega_h} \frac{1}{R_{x_0}} \nabla u_h \cdot \nabla v dx dy dz + \int \int \int_{\Omega_{H-h}} \frac{1}{R_t} \nabla u_h \cdot \nabla v dx dy dz = Iv|_{\Gamma_0}, \quad \forall v \in V. \quad (8.8)$$

By (8.6) and (8.8), we have

$$J_h(u_h) = -\frac{1}{2} I u_h|_{\Gamma_0} = -\frac{1}{2} \left( \int \int \int_{\Omega_h} \frac{1}{R_{x_0}} |\nabla u_h|^2 dx dy dz + \int \int \int_{\Omega_{H-h}} \frac{1}{R_t} |\nabla u_h|^2 dx dy dz \right). \quad (8.9)$$

Let  $U = u_h|_{\Gamma_0}$ . Keeping the other factors fixed,  $U$  is a function of  $h \in [0, H]$ , denoted by

$$U = U(h). \quad (8.10)$$

Since  $I > 0$ , by maximum principle it is evident that

$$U(h) > 0, \quad \forall h \in [0, H]. \quad (8.11)$$

For  $h, \tilde{h} \in [0, H]$  with  $\tilde{h} > h$ , let  $u_h \in V$ ,  $u_{\tilde{h}} \in V$  be the solutions of (8.7) corresponding to  $h = h$  and  $h = \tilde{h}$  respectively, i.e.,

$$J_h(u_h) = \min_{v \in V} J_h(v), \quad (8.12)$$

$$J_{\tilde{h}}(u_{\tilde{h}}) = \min_{v \in V} J_{\tilde{h}}(v). \quad (8.13)$$

Noting (8.3), it is easy to see from (8.9) and (8.12) that

$$\begin{aligned}
U(\tilde{h}) - U(h) &= \frac{2}{I}(J_h(u_h) - J_{\tilde{h}}(u_{\tilde{h}})) \\
&\leq \frac{2}{I}(J_h(u_{\tilde{h}}) - J_{\tilde{h}}(u_{\tilde{h}})) \\
&= \frac{2}{I}\left(\frac{1}{R_t} - \frac{1}{R_{x_0}}\right) \int \int \int_{\Omega_{\tilde{h}} \cap \Omega_{H-h}} |\nabla u_{\tilde{h}}|^2 dx dy dz \leq 0. \quad (8.14)
\end{aligned}$$

Actually, the strict inequality should hold in (8.14), since by Holmgren's uniqueness theorem (see [18]) it is impossible to have

$$\int \int \int_{\Omega_{\tilde{h}} \cap \Omega_{H-h}} |\nabla u_{\tilde{h}}|^2 dx dy dz = 0. \quad (8.15)$$

Thus, we have

$$U(\tilde{h}) < U(h), \quad \forall h, \tilde{h} \in [0, H] \text{ with } \tilde{h} > h, \quad (8.16)$$

namely,  $U(h)$  is a strictly decreasing function of  $h \in [0, H]$ .

It is easy to see that

$$\int \int \int_{\Omega} |\nabla u_h|^2 dx dy dz \leq C, \quad \forall h \in [0, H], \quad (8.17)$$

where  $C$  is a positive constant independent of  $h$ .

On the other hand, it follows from (8.8) that

$$U(\tilde{h}) - U(h) = \frac{1}{I}\left(\frac{1}{R_t} - \frac{1}{R_{x_0}}\right) \int \int \int_{\Omega_{\tilde{h}} \cap \Omega_{H-h}} \nabla u_{\tilde{h}} \cdot \nabla u_h dx dy dz \quad (\tilde{h} > h), \quad (8.18)$$

then by the absolute continuity of Lebesgue integration, for any fixed  $h \in [0, H]$ , we have

$$U(\tilde{h}) \rightarrow U(h) \text{ as } \tilde{h} \rightarrow h^+. \quad (8.19)$$

Similarly, for any fixed  $h \in (0, H]$ , we have

$$U(\tilde{h}) \rightarrow U(h) \text{ as } \tilde{h} \rightarrow h^-. \quad (8.20)$$

Hence  $U(h)$  is a continuous function of  $h \in [0, H]$ .

Since  $U = U(h)$  is a continuous and strictly decreasing function of  $h$  on  $[0, H]$ , it has a continuous and strictly decreasing inverse function  $h = h(U)$  for  $U \in [U(H), U(0)]$ . Hence, for each  $\bar{U} \in [U(H), U(0)]$ , the identification problem  $(P_h)$  admits a unique solution  $(\bar{h}, u_{\bar{h}}(x, y))$  with  $\bar{h} = h(\bar{U})$ .



In a similar way we can obtain the well-posedness for a single physical parameter identification. For example, we want to identify the resistivity  $R_t$ , provided that the other parameters are all known. Let

$$J_R(v) = \frac{1}{2} \left( \int \int \int_{\Omega_m} \frac{1}{R_m} |\nabla v|^2 dx dy dz + \int \int \int_{\Omega_{xo}} \frac{1}{R_{xo}} |\nabla v|^2 dx dy dz + \int \int \int_{\Omega_s} \frac{1}{R_s} |\nabla v|^2 dx dy dz + \int \int \int_{\Omega_t} \frac{1}{R_t} |\nabla v|^2 dx dy dz \right) - I v |_{\Gamma_0} \quad (8.21)$$

and  $V$  be defined by (8.5). The identification problem  $(P_R)$  to identify the resistivity  $R_t$  can be written in the following variational form: to find  $(R_t, u_{R_t}) \in (0, +\infty) \times V$  such that

$$\begin{cases} J_{R_t}(u_{R_t}) = \min_{v \in V} J_{R_t}(v), \\ u_{R_t} |_{\Gamma_0} = \bar{U}, \end{cases} \quad (8.22)$$

where  $\bar{U}$  is a given measuring potential on the electrode.

For any fixed  $R \in (0, +\infty)$ , there exists a unique  $u_R \in V$  such that

$$J_R(u_R) = \min_{v \in V} J_R(v). \quad (8.23)$$

Denoting  $U = u_R |_{\Gamma_0}$ ,  $U$  is a function of  $R \in (0, +\infty)$ :

$$U = U(R). \quad (8.24)$$

In a similar way, we can show that  $U = U(R)$  is a strictly decreasing and continuous function and

$$\begin{cases} \lim_{R \rightarrow 0} U(R) = U_0, \\ \lim_{R \rightarrow +\infty} U(R) = U_\infty, \end{cases} \quad (8.25)$$

where  $U_0$  or  $U_\infty$  is the measuring potential on the electrode in the case that  $\Omega_{R_t}$  is either a very good conductor or an insulator respectively. Thus for each  $\bar{U} \in (U_\infty, U_0)$  the identification problem  $(P_R)$  is well-posed.

For the multi-parameter identification, no good theoretical result has been obtained yet.

As shown in Fig.5.3, the results obtained by solving many direct problems for micro-spheric focusing well-logging can be plotted into a chart. By using that chart it is easy to graphically determine both the thickness of the mud-cake and the resistivity in the invaded zone by measuring  $I_0$  and  $I_1$ .

Tikhonov's regularization technique [19] and the pluse-spectrum technique [20] have been used to solve the identification problem for two parameters.

## 9 Boundary homogenization for inverse problems

When we use the patched electrode described in Section 7, it is interesting to investigate the limiting behaviour for the solution to the identification problem. Tan [21], Li & Tan [17] obtained the homogenization results for a single physical or geometric parameter identification respectively.

Suppose that an electrode is replaced by a patched electrode as in Section 7:

$$\Gamma_0 = \Gamma_0^\varepsilon \cup \tilde{\Gamma}_0^\varepsilon, \quad (9.1)$$

where  $\Gamma_0$  is the surface of the original electrode;  $\tilde{\Gamma}_0^\varepsilon$  is the insulator surface of the patched electrode and  $\Gamma_0^\varepsilon$  is the union of all the electrode cells:

$$\Gamma_0^\varepsilon = \bigcup_{i=1}^{m(\varepsilon)} \Gamma_{0,i}^\varepsilon. \quad (9.2)$$

For any fixed  $\varepsilon > 0$ , when the potential on  $\Gamma_0^\varepsilon$  is known:  $U = \bar{U}$ , we consider the following identification problem ( $P_h^\varepsilon$ ): to find  $(h^\varepsilon, u_{h^\varepsilon}^\varepsilon) \in [0, H] \times V_\varepsilon$  such that

$$\begin{cases} J_{h^\varepsilon}^\varepsilon(u_{h^\varepsilon}^\varepsilon) = \min_{v \in V_\varepsilon} J_{h^\varepsilon}^\varepsilon(v), \\ u_{h^\varepsilon}^\varepsilon = \bar{U} \text{ on } \Gamma_0^\varepsilon, \end{cases} \quad (9.3)$$

where

$$J_h^\varepsilon(v) = \frac{1}{2} \left( \int \int \int_{\Omega_h} \frac{1}{R_{xo}} |\nabla v|^2 dx dy dz + \int \int \int_{\Omega_{H-h}} \frac{1}{R_t} |\nabla v|^2 dx dy dz - I v|_{\Gamma_0^\varepsilon} \right) \quad (9.4)$$

and

$$V_\varepsilon = \{v \in H^1(\Omega) \mid v|_{\Gamma_1} = 0, v|_{\Gamma_0^\varepsilon} = \text{const}\} \quad (9.5)$$

with  $\Omega_h$  and  $\Omega_{H-h}$  defined in Section 8.

For each  $h \in [0, H]$  there exists a unique  $u_h^\varepsilon \in V_\varepsilon$  such that

$$J_h^\varepsilon(u_h^\varepsilon) = \min_{v \in V_\varepsilon} J_h^\varepsilon(v). \quad (9.6)$$

Let

$$U = u_h^\varepsilon|_{\Gamma_0^\varepsilon}. \quad (9.7)$$

$U$  is a function of  $h \in [0, H]$ , denoted by

$$U = U^\varepsilon(h), \quad (9.8)$$

provided that the other factors are all fixed. By the conclusion in Section 8,  $U^\varepsilon(h)$  is a continuous, strictly decreasing function of  $h \in [0, H]$  and

$$U^\varepsilon(h) > 0, \quad \forall h \in [0, H]. \quad (9.9)$$

So for any given  $\varepsilon > 0$ ,  $U = U^\varepsilon(h)$  has a continuous, strictly decreasing inverse function

$$h = h^\varepsilon(U), \quad \forall U \in [U(H), U(0)] \quad (9.10)$$

and the solution to identification problem  $(P_h^\varepsilon)$  for any given  $\bar{U} \in [U(H), U(0)]$  is given by  $(\bar{h}^\varepsilon, u_{\bar{h}^\varepsilon}^\varepsilon)$ , where

$$\bar{h}^\varepsilon = h^\varepsilon(\bar{U}). \quad (9.11)$$

Now we shall show that for the same measuring potential value  $\bar{U}$  on the electrode the solution  $(\bar{h}^\varepsilon, u_{\bar{h}^\varepsilon}^\varepsilon)$  to identification  $(P_h^\varepsilon)$  converges to the solution to identification problem  $(P_h)$  mentioned in §8, as  $\varepsilon \rightarrow 0$ .

Let  $U = U(h)$  be the potential value on the original electrode, which depends on the depth of the invaded zone as defined in Section 8. It is not difficult to show that

$$U^\varepsilon(h) > U(h). \quad (9.12)$$

By the homogenization result for the direct problem, for each  $h \in [0, H]$ , as  $\varepsilon \rightarrow 0$  we have

$$u_h^\varepsilon \rightarrow u_h \quad \text{strongly in } H^1(\Omega) \quad (9.13)$$

and

$$U^\varepsilon(h) \rightarrow U(h). \quad (9.14)$$

Noticing (9.12) and the strictly decreasing property of the inverse function we have

$$\bar{h}^\varepsilon > \bar{h}, \quad (9.15)$$

where  $\bar{h}^\varepsilon = h^\varepsilon(\bar{U})$  and  $\bar{h} = h(\bar{U})$ ,  $h(U)$  being the inverse function of  $U = U(h)$ . Under hypothesis (H) we shall show that for each  $\bar{U} \in (U(H), U(0)]$ ,

$$\bar{h}^\varepsilon \rightarrow \bar{h} \quad (9.16)$$

and

$$u_{\bar{h}^\varepsilon}^\varepsilon \rightarrow u_{\bar{h}} \quad \text{strongly in } H^1(\Omega) \quad (9.17)$$

as  $\varepsilon \rightarrow 0$ . In fact, since

$$J_h^\varepsilon(u_h^\varepsilon) = -\frac{1}{2} I u_h^\varepsilon|_{\Gamma_0^\varepsilon} = -\frac{1}{2} \left( \int \int \int_{\Omega_h} \frac{1}{R_{x_0}} |\nabla u_h^\varepsilon|^2 dx dy dz + \int \int \int_{\Omega_{H-h}} \frac{1}{R_t} |\nabla u_h^\varepsilon|^2 dx dy dz \right) \quad (9.18)$$

and

$$u_{\bar{h}^\varepsilon}^\varepsilon|_{\Gamma_0^\varepsilon} = \bar{U}, \quad (9.19)$$

we conclude that

$$\|u_{\bar{h}}^\varepsilon\|_{H^1(\Omega)} \leq C, \quad (9.20)$$

where  $C$  is a positive constant independent of  $\varepsilon$ . Then, by weak compactness and noticing  $0 \leq \bar{h}^\varepsilon \leq H$  we get that there exists a subsequence  $\varepsilon_n \rightarrow 0$  such that

$$\bar{h}^{\varepsilon_n} \rightarrow \tilde{h}, \quad (9.21)$$

$$u_{\bar{h}^{\varepsilon_n}}^{\varepsilon_n} \rightarrow \tilde{u} \text{ weakly in } H^1(\Omega), \quad (9.22)$$

$$u_{\bar{h}^{\varepsilon_n}}^{\varepsilon_n}|_{\Gamma_0} \rightarrow \tilde{u}|_{\Gamma_0} \text{ strongly in } L^2(\Gamma_0) \quad (9.23)$$

for some real number  $\tilde{h}$  and some function  $\tilde{u} \in H^1(\Omega)$  which satisfies

$$\int \int \int_{\Omega_{\tilde{h}}} \frac{1}{R_{x_0}} \nabla \tilde{u} \cdot \nabla v \, dx dy dz + \int \int \int_{\Omega_{H-\tilde{h}}} \frac{1}{R_t} \nabla \tilde{u} \cdot \nabla v \, dx dy dz = I v|_{\Gamma_0}, \quad \forall v \in V. \quad (9.24)$$

On the other hand, we have (at least for a subsequence of  $\varepsilon_n$ , still denoted by  $\varepsilon_n$ )

$$\chi_{\varepsilon_n} u_{\bar{h}^{\varepsilon_n}}^{\varepsilon_n}|_{\Gamma_0} \rightarrow \chi \tilde{u}|_{\Gamma_0} \text{ weakly in } L^2(\Gamma_0) \quad (9.25)$$

and

$$\chi_{\varepsilon_n} u_{\bar{h}^{\varepsilon_n}}^{\varepsilon_n}|_{\Gamma_0} = \chi_{\varepsilon_n} \bar{U} \rightarrow \chi \bar{U} \text{ weak star in } L^\infty(\Gamma_0). \quad (9.26)$$

Then, by hypothesis (H), we have

$$\tilde{u}|_{\Gamma_0} = \bar{U} \quad (9.27)$$

and then  $\tilde{u}$  is the solution to the direct problem with the depth of the invaded zone  $h = \tilde{h}$ . Because of the uniqueness of the solution to identification problem  $(P_h)$ , we have

$$\tilde{h} = \bar{h} = h(\bar{U}) \quad (9.28)$$

and

$$\tilde{u} = u_{\bar{h}}. \quad (9.29)$$

By noticing the convergence of the  $H^1$  norm of  $\{u_{\bar{h}^{\varepsilon_n}}^{\varepsilon_n}\}$  as  $\varepsilon \rightarrow 0$  and the uniqueness of the solution to the variational problem, finally we get (9.16)-(9.17).

In the case for identifying a single physical parameter, we have a similar result, i.e., for the same measuring value  $\bar{U}$  the identification result for the patched electrode tends to the identification result for the original electrode as  $\varepsilon$  tends to zero, provided that the total current discharged from these two kinds of electrodes are the same.

## 10 Other applications and generalization

The total flux boundary value problem which has been used to describe the resistivity well-logging electric field can be also applied to many other fields. For example, the temperature distribution around a cable where the total heat flux from unit length of the cable is known can be formulated by a boundary value problem with total flux boundary condition for the Laplace equation.

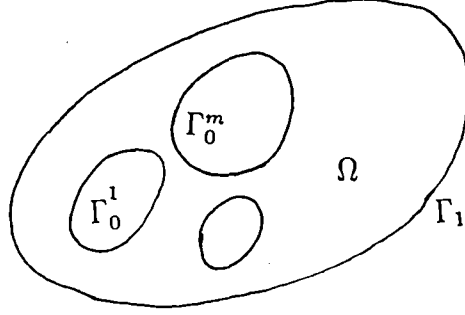


Figure 10.1

The most interesting problem is the torsion problem for an elastic rod with a multiply-connected cross section [22-23]. Let the cross section of the rod be shown as in Fig.10.1 and the stress function be

$$\Phi = 2G\theta\phi(x, y),$$

where  $G$  is the shear modulus and  $\theta$  is the torsion angle per unit length,  $\phi$  satisfies

$$-\Delta\phi = 1 \quad \text{in } \Omega \quad (10.1)$$

and

$$\phi = 0 \quad \text{on the exterior boundary } \Gamma_1. \quad (10.2)$$

Suppose that there are  $m$  holes with boundaries  $\Gamma_0^i (i = 1, \dots, m)$  in the cross section of the rod, then on each  $\Gamma_0^i$  we have the following total flux boundary condition

$$\begin{cases} \phi = C_i \text{ (unknown constant),} \\ \int_{\Gamma_0^i} \frac{\partial \phi}{\partial n} ds = A_i, \end{cases} \quad (10.3)$$

where  $A_i$  is the area of the  $i$ -th hole and  $n$  is the unit normal vector pointed to the interior of the hole. The theoretical and numerical method for the resistivity well-logging can be used to solve the torsion problem for this kind of rod.

The total flux boundary value problem can be extended to the time-dependence problem, i.e., to the evolution case. In petroleum exploitation, the oil pressure

$p = p(x, y, z)$  satisfies the equation

$$\frac{\partial p}{\partial t} - \Delta p = 0, \quad (10.4)$$

and the following boundary condition on the well-wall  $\Gamma_0$  [24-25]

$$\begin{cases} p = C(t) \text{ (unknown function of } t \text{) on } \Sigma_0 = \Gamma_0 \times (0, T), \\ \int_{\Gamma_0} \frac{\partial p}{\partial n} dS = A_0(t), \text{ for } t \in (0, T), \end{cases} \quad (10.5)$$

where  $A_0(t)$  is a given function which stands for the rate of oil flux per unit length from the wall at time  $t$ . Similar boundary condition can be also prescribed for the wave equation [27] and for the pseudo-parabolic equation [31]

$$(1 - \Delta) \frac{\partial u}{\partial t} - \Delta u = F(x, t). \quad (10.6)$$

The limiting behaviour of the solution to the time-dependant problem has been investigated in [26-28] with applications in the pointwise control [29-30].

The total flux boundary condition or the boundary condition with equivalued surface can be generalized to the so-called *complementary boundary condition* for the Laplace equation or for the Poisson equation:

$$\begin{cases} u - f \in M, \\ \frac{\partial u}{\partial n} - g \in M^\perp \end{cases} \quad (10.7)$$

on some boundary  $\Gamma_0$ , where  $f$  and  $g$  are given functions defined on  $\Gamma_0$ ,  $M$  is a closed subspace of  $H^{1/2}(\Gamma_0)$ ,  $M^\perp$  denotes the dual orthogonal complement of  $M$ , i.e.,

$$M^\perp = \{v \mid v \in (H^{1/2}(\Gamma_0))', \langle v, \phi \rangle_{((H^{1/2}(\Gamma_0))', H^{1/2}(\Gamma_0))} = 0, \forall \phi \in M\}, \quad (10.8)$$

in which  $(H^{1/2}(\Gamma_0))'$  denotes the dual space of  $H^{1/2}(\Gamma_0)$ .

By the variational method, it is easy to see that the corresponding *complementary boundary value problem* is well-posed [32]. Choosing  $M$  in different ways, we can obtain a great many boundary conditions, for example:

If  $M = \{0\}$  or  $M = H^{1/2}(\Gamma_0)$  we obtain the standard boundary condition of Dirichlet or of Neumann type respectively. Those are two extreme cases.

If  $M$  is a subspace spanned by  $\{1\}$ , i.e.,  $M = \{C\}$  where  $C$  is an arbitrary constant, and  $f \equiv 0$ , we obtain the total flux boundary condition.

If  $M$  is a subspace spanned by several linearly independent functions  $\phi_i (i = 1, \dots, J)$  in  $H^{1/2}(\Gamma_0)$ , and  $f \equiv 0$ , we obtain the following boundary condition:

$$u = \sum_{i=1}^J c_i \phi_i, \quad (i = 1, \dots, J) \quad (10.9)$$

and

$$\int_{\Gamma_0} \frac{\partial u}{\partial n} \phi_i dS = A_i \text{ (given constant), } (i = 1, \dots, J), \quad (10.10)$$

where  $c_i (i = 1, \dots, J)$  are unknown constants.

If  $M^\perp$  is a subspace spanned by  $\{1\}$  i.e.,  $M^\perp = \{C\}$  where  $C$  is an arbitrary constant, and  $g \equiv 0$ , we obtain the following nonlocal boundary condition

$$\frac{\partial u}{\partial n} = d \text{ (unknown constant)} \quad (10.11)$$

and

$$\int_{\Gamma_0} u dS = B \text{ (given constant).} \quad (10.12)$$

If  $M^\perp$  is a subspace spanned by several linear independent functions  $\psi_i (i = 1, \dots, K)$  in  $(H^{1/2}(\Gamma_0))'$ , and  $g \equiv 0$ , we obtain the boundary condition on  $\Gamma_0$  as follows:

$$\frac{\partial u}{\partial n} = \sum_{i=1}^K d_i \psi_i, \quad (i = 1, \dots, K) \quad (10.13)$$

and

$$\int_{\Gamma_0} u \psi_i dS = B_i \text{ (given constant), } (i = 1, \dots, K), \quad (10.14)$$

where  $d_i (i = 1, \dots, K)$  are unknown constants.

The complementary boundary value problem can be also extended into the evolution equations and the higher order equations [33-34].

## References

- [1] Zhang Geng-ji, *Electric Well-logs* (in Chinese), Oil Industry Press, Beijing, 1984.
- [2] Log Interpretation Charts, SCHLUMBERGER (1986).
- [3] Li Ta-tsien et al., Boundary value problems with equivalued surface boundary conditions for self-adjoint elliptic differential equations I (in Chinese), Fudan J. (Nat. Sci.), 1(1976), 61-71.
- [4] Li Ta-tsien et al., Boundary value problems with equivalued surface condition for self-adjoint elliptic differential equations II (in Chinese), Fudan J. (Nat. Sci.), 3-4(1976), 136-145.
- [5] Li Ta-tsien et al., *Applications of the Finite Element Method to Electric Well-logs* (in Chinese), Oil Industry Press, Beijing, 1980.

- [6] P.G.Ciarlet, *The finite element method for elliptic problems*, North-Holland publishing Co., Amsterdam. New York. Oxford, 1978.
- [7] Yu Wenci & Tan Yongji, The geometric quantity representation for FEM equations, *Math. in Practice & Theory.*, 1(1985), 54-64.
- [8] Li Ta-tsien et al., An examination of performance of the pole-panel of micro, spheric focussing log by computers (in Chinese), *Acta Math.Appl. Sinica*, 1(1979), 13-24.
- [9] Li Ta-tsien & Chen Shu-xing, On the asymptotic behavior of solutions to equivalued surface boundary value problems for the second order self-adjoint elliptic equation (in Chinese). *Fudan J. (Nat. Sci.)*, 4(1978), 6-14.
- [10] Sun Lianyou, Limiting behaviour for a class of equally valued boundary value problems and their applications to electric well-logging (in Chinese), *App. Math., J. of Chinese Univ., Ser. A*, 2(1993), 176-182.
- [11] Wei Ting, Theoretical analysis of mathematical models in well-logging (in Chinese), *Chin. Ann. of Math., Ser. A*, 13(1992), 664-671.
- [12] A.Damlamian & Li Ta-tsien, Homogénéisation sur le bord pour des problèmes elliptiques, *C.R.Acad.Sci.Paris, Sér. I*, 299(1984), 859-862.
- [13] A.Damlamian & Li Ta-tsien, Boundary homogenization for elliptic problems, *J.Math.Pures et Appl.*, 66(1987), 351-361.
- [14] Li Ta-tsien, Nonlocal boundary value problems and homogenization of boundary conditions, *International Workshop on Applied Differential Equations*, World Scientific, 1986, 267-275.
- [15] J. Sylvester and G. Uhlmann., A uniqueness theorem for an inverse boundary value problem in electrical prospection, *Comm. Pure Appl. Math.*, 39 (1986), 92-112.
- [16] Tan Yongji, An inverse problem for nonlocal BVP and resistivity identification, *Partial Differential Equations (Proceeding, Tianjin, 1986, edited by S.S.Chern)*, *Lecture Notes in Math.* 1306, Springer-verlag, 1988, 149-159.
- [17] Li Ta-tsien & Tan Yongji, Some identification problems in petroleum geophysics, *Control of Boundaries and Stabilization (Proc. IFIP Conference, Clermont Ferrand, France)* *Lecture Notes in Control and Information Sciences* 125, Springer-Verlag, 1989, 199-210.



- [18] F.Treves, *Basic Linear Partial Differential Equations*, Academic Press, Inc., 1975.
- [19] Bai Donghua et al, The mathematical inversion for the side way logging (in Chinese), J. of Sichuan Univ, 3(1992), 359-369.
- [20] Liu Jia-qi et al, An iterative algorithm for solving the resistivity of the earth and the diameter of the invaded zone simultaneously (in Chinese), J. Geophysics 32, 4(1989), 434-440.
- [21] Tan Yongji, Boundary homogenization of an inverse non-local elliptic boundary value problem, IMA J. of Appl. Math., 41(1988), 135-146.
- [22] Li Ta-tsien, Elastic torsion of bars with multiply-connected cross section (in Chinese), Comm. Appl. Math. Comput. 1(1987), 19-24.
- [23] Li Ta-tsien, A class of non-local boundary value problems for partial differential equations and its applications in numerical analysis, J. Comp. Appl. Math., 28(1989), 49-62.
- [24] Shen Weixi, On mixed initial-boundary value problems of second order parabolic equations with equivalued surface boundary conditions, Fudan J.(Nat.Sci.), 4(1978), 15-24.
- [25] Chen Zong-xiang & Jiang Li-shang, Exact solution for the system of flow equations through a medium with double-porosity, Sci.Sinica, 7(1980), 880-896.
- [26] A.Damlamian & Li Ta-tsien, Comportements limites des solutions de certains problèmes mixtes pour des équations paraboliques, C.R.Acad.Sc.Paris, Ser A, 290(1980), 957-960; J. Math. Pures et Appl., 61(1982), 113-130.
- [27] A.Damlamian & Li Ta-tsien, Comportements limites des solutions de certains problèmes mixtes pour des équations hyperboliques linéaires, C.R.Acad. Paris, Ser A, 291(1980), 531-534; Comm. Partial Differential Equations, 2(1982), 117-139.
- [28] A.Damlamian & Li Ta-tsien, Comportement limite des solutions de certains problèmes mixtes pour des équations paraboliques II, Acta Math. Sci. 2(1982), 85-104.
- [29] Li Ta-tsien, Comportements limites pour certain problèmes du contrôle optimal de systèmes gouvernés par des équations paraboliques, C.R.Acad.Sc. Paris, Ser. A, 291(1980), 201-204.

- [30] J.L.Lions, *Some Methods in the Mathematical Analysis of Systems and their Control*, Science Press, Beijing, 1981.
- [31] Li Ta-tsien & L. W. White, Total flux(nonlocal) boundary value problems for pseudoparabolic equations, *Applicable Anal.*, 1(1983), 17-31.
- [32] Li Ta-tsien et al., Boundary value problems with complementary boundary conditions for self-adjoint elliptic equations (in Chinese), *Fudan J.(Nat.Sci.)*, 2(1978), 49-60.
- [33] Chen Shu-xing, On boundary value problems of the second order partial differential equation with complementary boundary conditions, *Fudan J.(Nat.Sci.)*, 4(1979), 37-44.
- [34] Chen Shu-xing, Nonlocal boundary value problems for the elliptic equation of higher order, *Acta Math. Sinica*, 2(1983), 163-170.

Authors' address: Prof. Li Ta-tsien and Prof. Tan Yongji, Department of Mathematics, Fudan University, Shanghai 200433, P.R.China.



---

Unité de Recherche INRIA Rocquencourt  
Domaine de Voluceau - Rocquencourt - B.P. 105 - 78153 LE CHESNAY Cedex (France)  
Unité de Recherche INRIA Lorraine Technopôle de Nancy-Brabois - Campus Scientifique  
615, rue du Jardin Botanique - B.P. 101 - 54602 VILLERS LES NANCY Cedex (France)  
Unité de Recherche INRIA Rennes IRISA, Campus Universitaire de Beaulieu 35042 RENNES Cedex (France)  
Unité de Recherche INRIA Rhône-Alpes 46, avenue Félix Viallet - 38031 GRENOBLE Cedex (France)  
Unité de Recherche INRIA Sophia Antipolis 2004, route des Lucioles - B.P. 93 - 06902 SOPHIA ANTIPOLIS Cedex (France)

---

EDITEUR  
INRIA - Domaine de Voluceau - Rocquencourt - B.P. 105 - 78153 LE CHESNAY Cedex (France)

ISSN 0249 - 6399

